ISSN 0006-2979, Biochemistry (Moscow), 2006, Vol. 71, No. 7, pp. 800-809. © Pleiades Publishing, Inc., 2006.
Original Russian Text © D. V. Mamaev, D. A. Aliverdieva, D. I. Bondarenko, K. F. Sholtz, 2006, published in Biokhimiya, 2006, Vol. 71, No. 7, pp. 984-995.
Originally published in Biochemistry (Moscow) On-Line Papers in Press, as Manuscript BM06-022, June 4, 2006.

# Study of Active Site Topography of Rat Liver Mitochondrial Dicarboxylate Transporter Using Lipophilic Substrate Derivatives

**D. V. Mamaev[1], D. A. Aliverdieva[2]*, D. I. Bondarenko[1], and K. F. Sholtz[1]**

[1]*Bach Institute of Biochemistry, Russian Academy of Sciences, Leninsky pr. 33, 119071 Moscow, Russia*
[2]*Caspian Institute of Biological Resources, Dagestan Research Center, Russian Academy of Sciences, ul. Gadgieva 45, 367025 Makhachkala, Russia; E-mail: dinara0195@mail.ru*

Received January 30, 2006
Revision received March 27, 2006

**Abstract**—Earlier it has been demonstrated that the active site (substrate-binding site + active site channel) of rat liver mitochondrial dicarboxylate transporter is characterized by rather complex topography. Probing the active site with 2-monoalkylmalonates revealed the existence of internal and external lipophilic areas separated by a polar region. A two substrate-binding site model of the transporter has been supposed. The correctness of this model has been evaluated by probing the active site with O-acyl-L-malates differing from 2-monoalkylmalonates by 0.23 nm longer distance from the anion groups to the aliphatic chain. Changes in the polar group of the probe did not prevent its binding and showed the same variable lipophilicity pattern for the transporter channel. Probing with α,ω-alkylene dimalonates did not reveal the second substrate-binding site at the active site. The substrate-binding site did not show any differences in affinity to O-acyl-derivatives of L-malate and D-malate, except L-malate binds more effectively than D-malate. This suggests involvement of the L-malate hydroxyl group in substrate binding and stereospecific behavior of the transporter substrate-binding site. A modified one substrate-binding site model of the dicarboxylate transporter is discussed.

**DOI**: 10.1134/S0006297906070133

*Key words*: mitochondrial dicarboxylate transporter, succinate dehydrogenase, transport competitive inhibitors, 2-alkylmalonates, O-acyl-L- and D-malates, α,ω-alkylene dimalonates, substrate-binding site stereospecificity

The mitochondrial dicarboxylate carrier responsible for transport of L-malate, succinate, and phosphate plays an important role in cell metabolism [1]. The primary structure of mitochondrial dicarboxylate transporter has been elucidated for mouse [2], rat [3], the nematode *Caenorhabditis elegans* [3], the yeast *Saccharomyces cerevisiae* [4], and human [5]. So it has become possible to predict its secondary structure and to reveal invariant amino acid residues essential for dicarboxylate transport. It is suggested that the transporter functions as a homodimer and each subunit has six hydrophobic transmembrane segments joint by hydrophilic loops exposed to the mitochondrial matrix and cytoplasm [1, 5]. Perhaps, these segments form a transmembrane channel. Each segment has several polar amino acid residues, but it remains unclear whether they are exposed into the channel lumen. Primary structures of the family of mitochondrial carriers share high similarity (up 34% [6]), and this suggests similarity in their tertiary structures. The 3D structure has been obtained for adenylate transporter only, and it might represent a paradigm for other members of this protein family [7]. However, the resolution of X-ray analysis (2.2 Å) was not sufficient for identification of amino acid residues "lining" the transporter channel and for evaluation of lipophilicity of the channel walls.

Previously we analyzed the topography of the active site channel of rat liver mitochondrial dicarboxylate transporter using its competitive inhibitors, 2-monoalkyl malonates [8, 9]. Changes in $K_i$ values in response to elongation of these compounds by one methylene unit ($\Delta K_i = K_{i(n)} - K_{i(n-1)}$) characterized lipophilicity of the transporter region binding this group [9]. We found that the transporter channel has small and large lipophilic areas separated by a well-defined polar region. The former is positioned around the substrate-binding site, whereas the latter is located near the channel gate. The sizes of these areas were 0.38, not less than 0.88, and 0.50 nm in length, respectively. This means that the length of the external half-channel should not be less than

* To whom correspondence should be addressed.

1.76 nm. So we suggested that the substrate-binding site of this channel is located in the middle of the membrane [8] as the thickness of its hydrophobic core layer is assumed to be 4.0 nm.

Manipulations with some citrate [10], α-ketoglutarate [11], and adenylate [12] mitochondrial transporters have revealed that substitution of invariant arginine residues located in the depth of transmembrane segments is accompanied by irreversible loss of biological activity. Three conservative arginine residues of dicarboxylate transporter are located within the inner third of transmembrane segments II, IV, and VI [5], but only Arg72 of segment II is invariant for both of animals and yeasts [4]. It remains unclear which of these basic residues may be involved in formation of substrate-binding sites of this transporter.

In this study, we have investigated some features of the substrate-binding site of rat liver mitochondrial dicarboxylate carrier, its stereospecificity, and its environment using O-acyl-L-malates, 2-alkyl malonates, and O-acyl-D-malates. The number of substrate-binding sites was evaluated using α,ω-alkylene dimalonates as bifunctional reagents.

The rate of succinate transport was evaluated in tightly coupled rat liver mitochondria [8, 9, 13]. This excluded possible changes in properties of dicarboxylate carrier during its reconstitution into liposomes as has been demonstrated for tricarboxylate [14] and adenylate [15] transporters.

## MATERIALS AND METHODS

Rat liver mitochondria were isolated by the method of Weinbach [16]. Submitochondrial particles were obtained by the method of Pedersen et al. [17]. Protein content was determined by the method of Goa [18].

Mitochondrial incubation medium (medium M1) contained 125 mM sucrose, 20 mM Tris-HCl, pH 7.2, 2 mM EDTA, 20 mM KCl, 2.5 mM $MgCl_2$, and 10 mM $KH_2PO_4$. The incubation medium for mitochondria with damaged outer membrane (medium M2) contained 10 mM succinate, 2 mM EDTA, 2.5 mM $MgCl_2$, and 10 mM Tris, pH 7.2.

The rate of mitochondrial succinate oxidation was assayed polarographically using a cell with a covered electrode [19]. The media M1 and M2 were used for intact mitochondria and mitochondria with damaged outer membrane, respectively. In the case of M2 medium, 100 mM sucrose was added 1 min after addition of mitochondria to stop hypotonic shock [20].

The rate of the succinate:ferricyanide-reductase reaction was assayed in submitochondrial particles and M1 medium as described earlier [8]. Rotenone (final concentration 1 μM) was added just before the mitochondria. Concentrations of the protonophore 3,5-di-tert-butyl-4-hydroxybenzylidene malononitrile were varied depending on mitochondrial protein concentration and the partition coefficient of the protonophore [21]. The rate of mitochondrial 3-hydroxybutyrate oxidase reaction was assayed in M1 medium in the presence of 10 mM sodium hydroxybutyrate and the protonophore. The rate of mitochondrial respiration in the presence of transport inhibitors was assayed under steady-state conditions after reaching maximal effect.

Partition coefficients of O-acyl-L-malates ($R_n$) were determined after equilibration in the system octanol/water (phosphate buffer, pH 7.2) by assaying inhibitor concentrations in the aqueous phase with methylene blue [22]. The coefficient was calculated by the following formula: $R = (C_0 - C_w)v_w/C_w v_o$, where $C_0$ and $C_w$ are initial and equilibrium concentrations of a malate in the aqueous phase and $v_o$ and $v_w$ are volumes of octanol and water phases, respectively.

If apparent inhibition constant ($K_i°$) depended on mitochondrial concentration ($B$), true inhibition constant $K_i$ was determined by extrapolation to zero concentration of mitochondria using $K_i°$ versus $B$ plots as proposed by Heirwegh et al. [23]. This approach has been used for higher 2-alkyl malonates (starting from 2-dodecyl malonate) and higher O-acyl-L- and D-malates (starting from O-myristoyl malate) and also for 1,8-octylene dimalonate and 1,11-undecylene dimalonate). The dependence can be described by the following equation: $K_i° = K_i + (K_i R\lambda)$ [8]. The expression in parenthesis including partition coefficient between mitochondria and medium ($R$), specific volume of lipophilic phase susceptible to the inhibitor (λ), and $K_i$ is a constant.

The following chemicals were used in the study: protonophore 3,5-di-tert-butyl-4-hydroxybenzylidene malononitrile from Sumitomo Chem. Co. (Japan); rotenone, antimycin A, cytochrome *c*, and Tris from Serva (Germany); L- and D-malic acids from Sigma (USA); disodium salts of ADP and EDTA from Reanal (Hungary); sodium 3-hydroxybutyrate from Ferak (Germany); bovine serum albumin from Calbiochem (USA). Gramicidin S recrystallized from ethanol was obtained from Prof. G. F. Gause. Other chemicals were from local suppliers: $KH_2PO_4$ and KOH of specially pure grade; $MgCl_2$, $K_3Fe(CN)_6$, KCN, malonic acid, and sucrose of chemically pure grade; sodium succinate was recrystallized twice from water.

Derivatives of L-malate, D-malate, and malonate (2-alkyl malonates, 2,2-dialkyl malonates, O-acyl-L- and O-acyl-D-malates, α,ω-alkylene dimalonates) were synthesized in our laboratory. The resulting compounds were purified by multiple recrystallizations. Their purity was evaluated by gas–liquid chromatography (GLC) using Tsvet-102 (compounds were analyzed as methyl esters) or thin layer chromatography (TLC) using Silufol TLC plates (Czech Republic). Elemental analysis of the synthesized compounds corresponded to their structure.

## RESULTS

For assay of dicarboxylate transporter activity in intact mitochondria, we have used a coupled system of succinate oxidation (defined further as succinate oxidase). This system consists of the dicarboxylate transporter, succinate dehydrogenase complex (defined further as succinate dehydrogenase), and ubiquinol oxidase. The latter is a common component for succinate oxidase and 3-hydroxybutyrate oxidase. Earlier we demonstrated that concentrations of mono- and dialkyl malonates inhibiting succinate oxidation had a minor influence on 3-hydroxybutyrate oxidation [8, 24]. Similar results were obtained for O-acyl-L- and D-malates and also for α,ω-alkylene dimalonates (data not shown). This means that inhibitors influenced either transport of succinate or activity of succinate dehydrogenase. Among all malonate derivatives tested, only comparable concentrations of 2-methyl malonate inhibited both systems. However, the $IC_{50}$ value for mitochondrial succinate oxidase was more than one order of magnitude higher than that for submitochondrial particle succinate-ferricyanide reductase: 2.52 and 65.2 mM, respectively. (In both experiments 3 mM succinate was used.)

Figure 1 shows the effect of various concentrations of one O-acyl malate, O-lauroyl-L-malate, on succinate oxidase. Mitochondrial permeabilization by the channel-forming gramicidin S significantly reduced the inhibitory effect. The appearance of a plateau suggesting insensitivity of some proportion of succinate oxidase to this inhibitor may be attributed to the gramicidin S-induced succinate permeability independent of dicarboxylate transporter.

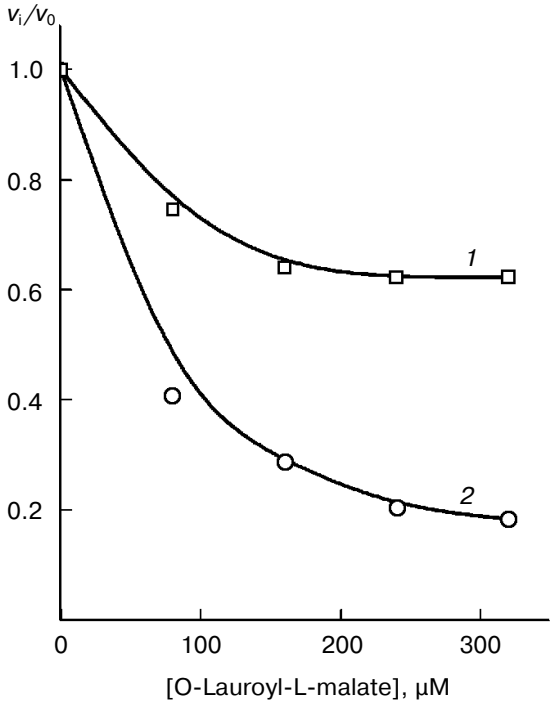


**Fig. 1.** Dependence of the rate of rat liver mitochondrial succinate oxidation assayed with (*1*) or without 2.25 μM gramicidin S (*2*) in the presence of 3 mM succinate and 4 μM cytochrome *c* on O-lauroyl-L-malate concentrations. Mitochondrial protein concentration was 0.2 mg/ml. Here and in Figs. 2-5, $v_0$ and $v_i$ are the rates in the absence and presence of the inhibitor, respectively.

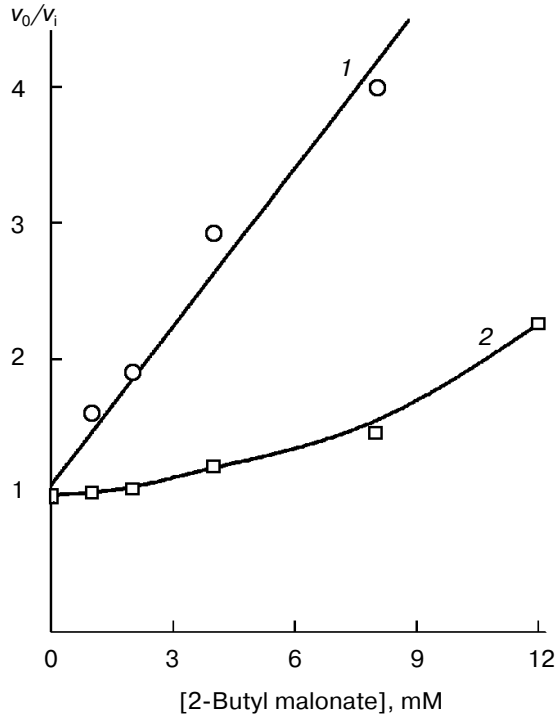


**Fig. 2.** Dependence of succinate oxidation by cytochrome *c* partially exhausted rat liver mitoplasts determined in the presence (*1*) and in the absence of 4 μM cytochrome *c* (*2*) on 2-butyl malonate concentration. Mitoplast protein concentration was 0.5 mg/ml.

Sublytic concentrations of gramicidin S are known to induce permeability of bacterial membranes for large ions [25]. Under our conditions, gramicidin S concentration was one order of magnitude less than the concentration required for cell lysis (2.5 and 40 μM, respectively). The presence of an uncoupler in the medium (Fig. 1) prevented mitochondrial swelling [26]. The plateau observed in the presence of gramicidin S means that O-lauroyl-L-malate either cannot reach the mitochondrial matrix in which succinate dehydrogenase is exposed or its action on the enzyme is much weaker than that on the dicarboxylate transporter. In the presence of gramicidin S (responsible for the transporter bypass) and 3 mM succinate, the rate of the succinate oxidase reaction increased by 17%. Such behavior may be due to activation of succinate dehydrogenase by some additional quantity of succinate penetrating into the matrix. A similar result (15% activation) was obtained in the presence of 10 mM succinate. This is the saturating concentration for both transporter and succinate dehydrogenase. Since transporter-independent succinate flux was not less than 50% (Fig. 1), the

activity of the coupled system exceeded transporter activity by at least 30%. Thus, under the conditions of our experiment succinate transport was the rate-limiting step for mitochondrial succinate oxidase. This is consistent with the data that rat liver mitochondrial succinate oxidase and isolated dicarboxylate transporter have similar affinity for succinate ($K_m$ values of 1.01 [8] and 1.17 mM [27], respectively) and 2-butyl malonate ($K_i$ values of 0.37 [8] and 0.4 mM [28], respectively).

In mitochondria with damaged outer mitochondrial membrane succinate oxidase activity decreased in reversible manner due to release of cytochrome *c* into the medium, and under these conditions ubiquinol oxidase became the rate-limiting factor [20]. Figure 2 shows that the change in the rate-limiting factor was accompanied by appearance of nonlinear dependence of succinate oxidation inhibition on 2-butyl malonate in Dixon plots. In the presence of excess cytochrome *c*, the linearity of inhibition was restored. This suggests that in the presence of the inhibitor the transporter remains the rate-limiting factor for succinate oxidase.

Linear behavior of Dixon plots was obtained for all inhibitors studied. Figures 3b-5b show such dependences for butyroyl-L-malate (member of acyl-L-malates), myristoyl-D-malate (member of acyl-D-malates), and for 1,11-undecylene dimalonate (member of α,ω-alkylene dimalonates). For mono- and dialkyl malonates such experiments have been carried out earlier [8, 24] (data not shown for L- and D-malate). Thus, under our experimental conditions $K_i$ value for succinate oxidase inhibition reflects affinity of the inhibitors tested for the dicarboxylate transporter.

Figure 3a shows that butyroyl- and stearoyl-L-malates, the marginal members of the acyl-L-malate series, increased $K_m$ value for mitochondrial succinate oxidase without influencing maximal rate value. Figures 4a and 5a demonstrate similar behavior of myristoyl-D-malate, the member of acyl-D-malates, and 1,11-undecylene dimalonate, the member of α,ω-alkylene dimalonates. The effects of mono- and dialkyl malonates were investigated earlier [8, 24] (for L- and D-malate data not shown). The competitive mode of interaction of these inhibitors suggests that they interact with substrate-binding site of the transporter active site.

Figure 6 shows the O-acyl-L-malates and 2-alkyl malonates exhibit similar behavior of the dependence of

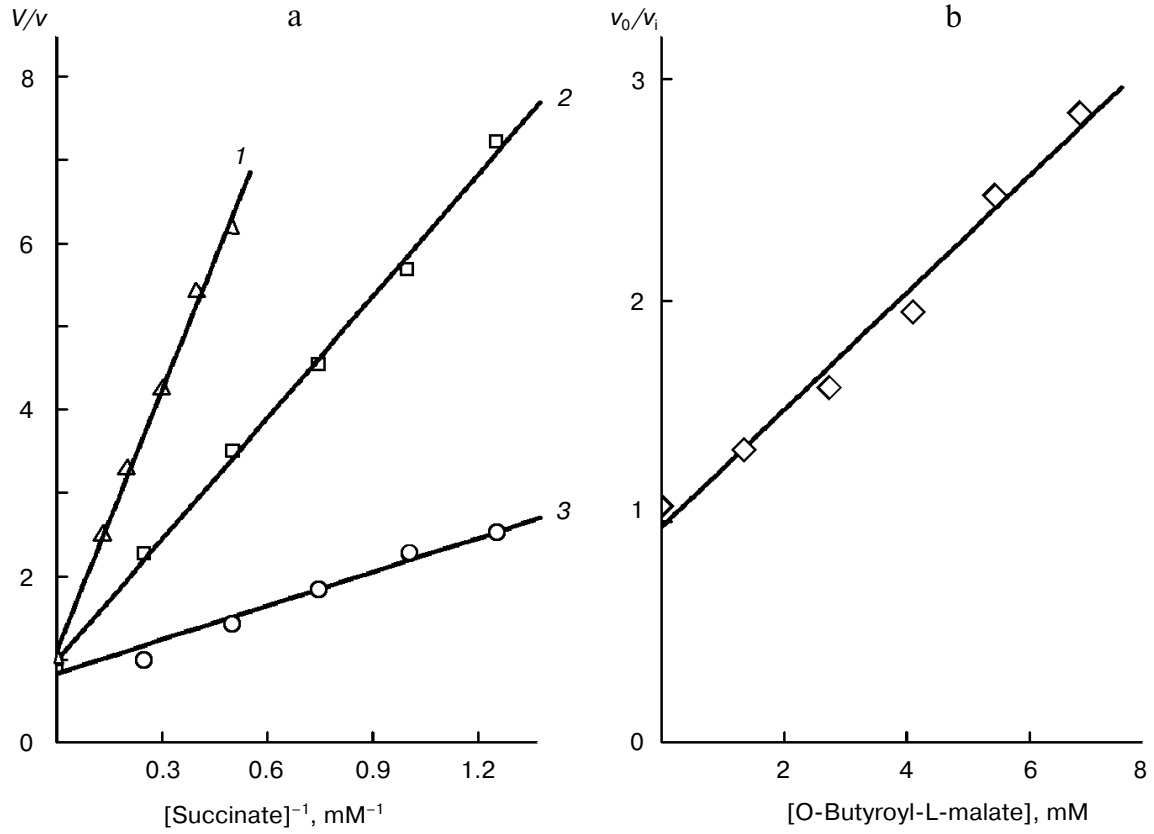


**Fig. 3.** a) Effect of 8 μM O-stearoyl-L-malate (*1*) and 6.8 mM O-butyroyl-L-malate (*2*) on the dependence of rat liver mitochondrial succinate oxidation on succinate concentration presented in Lineweaver–Burk plots; *3*) without inhibitor. Mitochondrial protein concentration was 0.5 mg/ml. b) Dixon plot of the dependence of inhibition of rat liver mitochondrial succinate oxidation by O-butyroyl-L-malate assayed with 3 mM succinate. Mitochondrial protein concentration was 0.5 mg/ml. Here and in Figs. 4 and 5, *V* is a maximal rate in the absence of the inhibitor and *v* is a rate at the given substrate concentration.

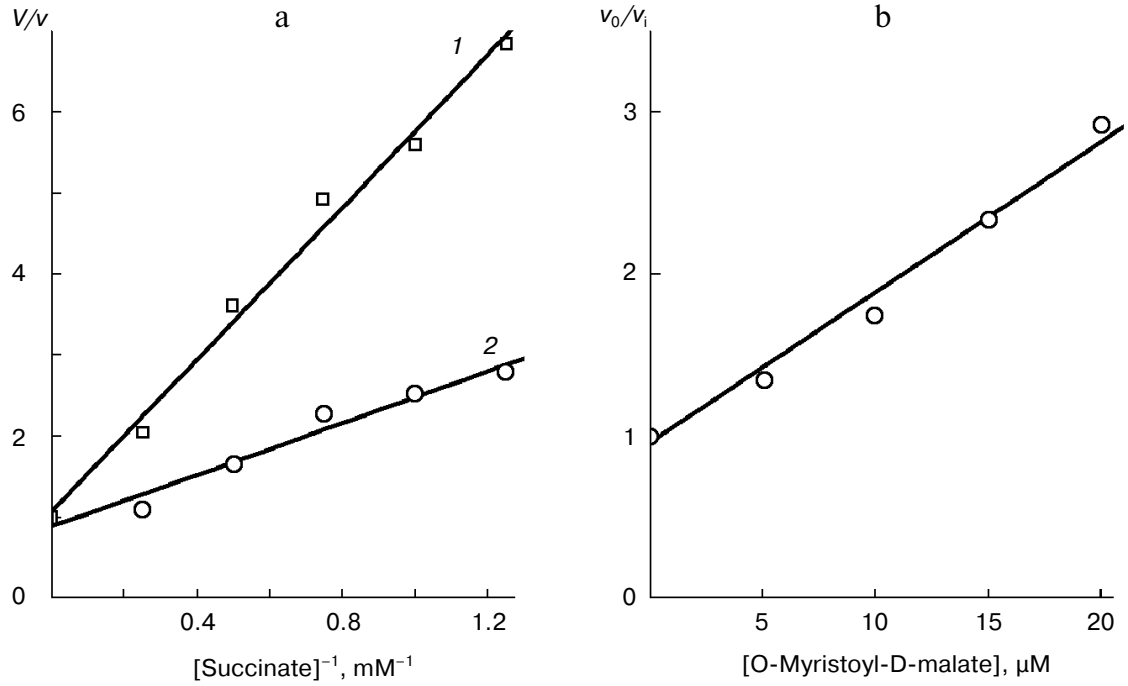


**Fig. 4.** a) Lineweaver–Burk plots of the dependence of rat liver mitochondrial respiration on succinate concentration in the presence (*1*) and in the absence of O-myristoyl-D-malate (*2*). b) Dixon plot of the dependence of rat liver mitochondrial respiration on the inhibitor concentration. Mitochondrial protein concentration and succinate concentration were 0.5 mg/ml and 3 mM, respectively.

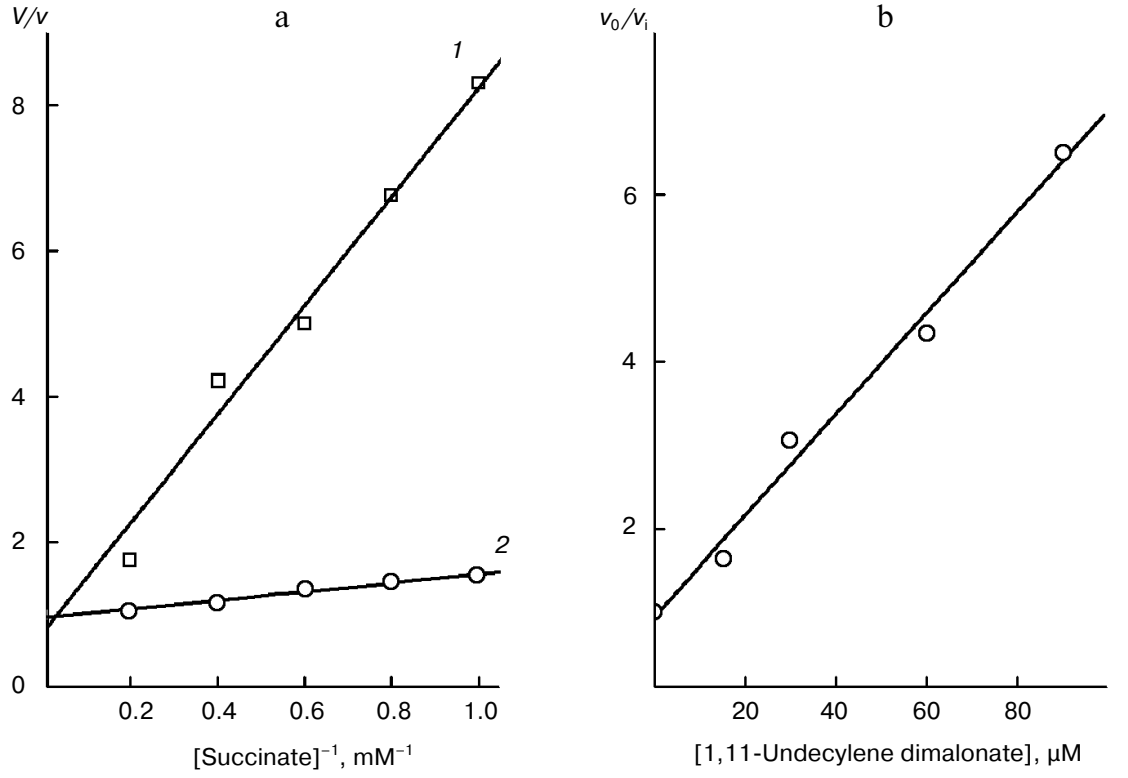


**Fig. 5.** a) Lineweaver–Burk plots of the dependence of rat liver mitochondrial respiration on succinate concentration in the presence (*1*) and in the absence of 62.5 μM 1,11-undecylene dimalonate (*2*). b) Dixon plot of the dependence of rat liver mitochondrial respiration on 1,11-undecylene dimalonate concentration. Mitochondrial protein concentration and succinate concentration were 0.5 mg/ml and 3 mM, respectively.

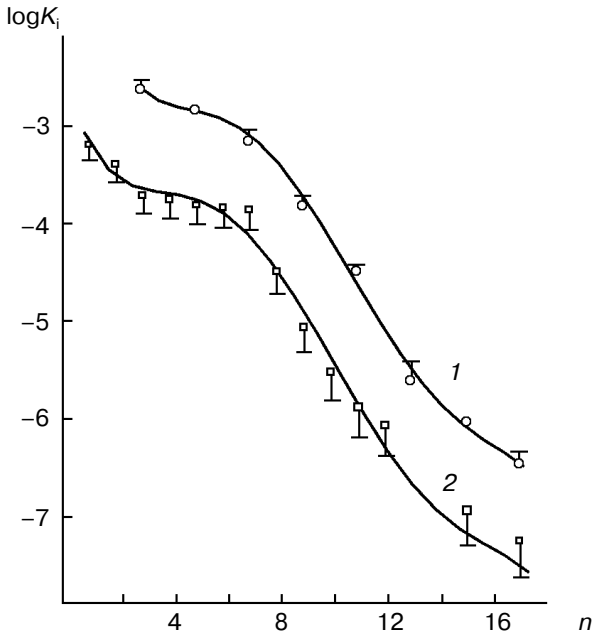


**Fig. 6.** Dependence of $K_i$ value for inhibition of rat liver mitochondrial succinate oxidase by O-acyl-L-malates (*1*) and 2-alkyl malonates (*2*) on the number of carbon atoms (*n*) in the aliphatic chain.

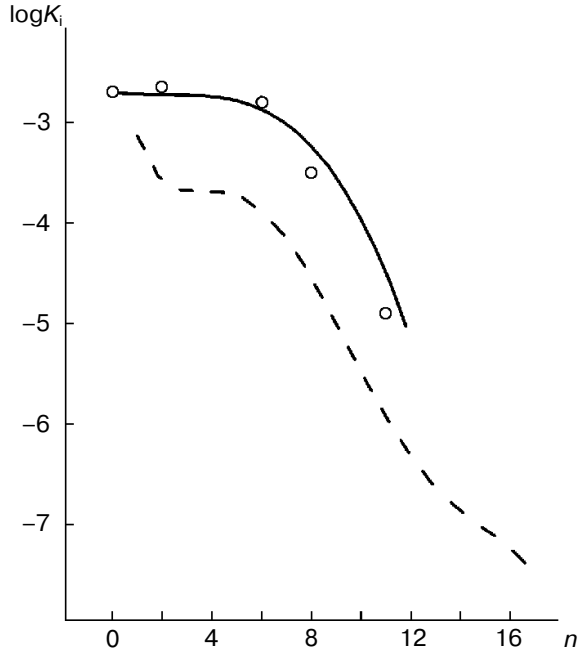


**Fig. 7.** Dependence of $K_i$ value for the inhibition of rat liver mitochondrial succinate oxidase by α,ω-alkylene dimalonates (solid curve) and 2-alkyl malonates (dashed curve) on the number of carbon atoms in the aliphatic chain.

$K_i$ values on *n*. Both curves are characterized by a plateau at *n* from 4 to 8 (binding to polar region) and the zone of reduced $K_i$ for *n* ranging from 8 to 15 (binding with large lipophilic region). It is possible that similar parts of the aliphatic chain of O-acyl-L-malates and 2-monoalkyl malonates bind at common regions of the transporter channel. A characteristic feature of the effect of O-acyl-L-malates on dicarboxylate transporter consists in the fact that their $K_i$ values are roughly one order of magnitude higher than $K_i$ values for 2-alkyl malonates of the same aliphatic chain length ($\Delta\log K_i = 1.2$). $K_i$ values for L-malate ($0.5 \pm 0.15$ mM) and malonate (0.35 mM [29]) are nearly the same.

We have previously demonstrated that mono- and dialkyl malonates are competitive inhibitors of succinate dehydrogenase [8] and mitochondrial dicarboxylate transporter [24]. Table 1 shows results of active site probing of succinate dehydrogenase and dicarboxylate transporter (sharing a common substrate, succinate) with these compounds. The presence of additional substituents near carboxyl groups caused more pronouncedly reduced affinity to the enzyme than to the transporter. This suggests that the region around the substrate-binding site of the transporter is rather large.

Figure 7 shows the dependence of $K_i$ value on the number of carbon atoms *n* of α,ω-alkylene dimalonates. It shares significant similarity with the corresponding dependence obtained for higher 2-alkyl malonates (Fig. 7, dashed line). This dependence has a characteristic plateau up to $n = 6$ and a region of decreased $K_i$ value at *n* ranging from 6 to 11. It is possible that methylene units of both groups of inhibitors positioned at equal distance from the substrate-binding site interact with the same areas of the transporter. Corresponding α,ω-alkylene dimalonates caused a weaker inhibition than 2-alkyl malonates. Interestingly, the half-period for reaching steady-state inhibition was 1 min for α,ω-alkylene dimalonates, and less than 10 sec for both 2-alkyl malonates and O-acyl-L-malates (data not shown).

The data of Table 2 show that $K_i$ value for mitochondrial succinate oxidase inhibition by D-malate is 5 times

**Table 1.** Dependence of $K_i$ value for the inhibition of rat liver succinate:ferricyanide reductase of submitochondrial particles and mitochondrial succinate oxidase on the number of carbon atoms in alkyl substituents of malonate derivatives (number of independent assays is shown in parentheses)

| Inhibitor | $-\log K_i$ for succinate oxidase | $-\log K_i$ for succinate dehydrogenase |
|---|---|---|
| Malonate | 3.7 [29] | $5.65 \pm 0.10$ (3) |
| 2-Methyl malonate | $3.20 \pm 0.2$ (3) | $2.72 \pm 0.19$ (2) |
| 2,2-Dimethyl malonate | $2.56 \pm 0.12$ (3) | $1.55 \pm 0.18$ (3) |

**Table 2.** Inhibition of rat liver mitochondrial succinate oxidase by O-acyl-L-malates and O-acyl-D-malates containing the same substituents (number of independent assays is shown in parentheses)

| Inhibitor | Number of methylene units in the aliphatic chain of inhibitor ($n$) | $-\log K_i$ |
|---|---|---|
| L-Malate | 0 | 3.3 ± 0.2 (2) |
| D-Malate | 0 | 2.6 ± 0.15 (3) |
| O-Myristoyl-L-malate | 13 | 5.5 ± 0.2 (3) |
| O-Myristoyl-D-malate | 13 | 5.22 ± 0.12 (2) |
| O-Stearoyl-L-malate | 17 | 6.4 ± 0.12 (2) |
| O-Stearoyl-D-malate | 17 | 6.6 ± 0.14 (2) |

higher than that for L-malate ($\Delta\log K_i = 0.7$). However, $K_i$ values for O-acyl derivatives of these stereoisomers insignificantly differed. This suggests involvement of hydroxyl group of L-malate in binding of this substrate in the active site of this transporter. Changes in spatial orientation of this group in the malate molecule or blockade of this group exclude such interaction. Half-periods for reaching steady-state rate for inhibition of succinate transport by D- and L-malate were 30 and less than 10 sec (data not shown). The derivatives of both stereoisomers were characterized by half-period of less than 10 sec. Since D- and L-malates are transported by the same transporter, different rates of inhibition by stereoisomers may reflect stereospecificity of this transport. Higher $K_i$ values for O-acyl-L-malates than those for 2-alkyl malonates ($\Delta\log K_i = 1.2$, see Fig. 6) may be explained by blockade of hydroxyl group in these compounds; however, involvement of some additional factors influencing inhibitory potency of malate and malonate derivatives is also possible.

## DISCUSSION

Using several independent approaches (Figs. 1, 2, 3b, 4b, and 5b) we have demonstrated that transport of succinate into mitochondria limits its oxidation by the succinate oxidase system in the presence and in the absence of the inhibitors studied: O-acyl-L- and D-malates, 2,2-dialkyl malonates, and α,ω-alkylene dimalonates. Dixon plots exhibited monophasic inhibitory behavior (Figs. 3b, 4b, and 5b). This suggests that all these inhibitors interact with the same protein, the dicarboxylate transporter. Analysis of the effects of these competitive inhibitors (Figs. 3a, 4a, and 5a) represents a good tool for investigation of the substrate-binding region (and its environment) of the active site.

Assuming that accommodation of all these effectors in the active site of dicarboxylate transporter requires the same active site conformation, differences in the inhibitory potency may be attributed to the features of the substrate binding region and its (micro)environment. Similar inhibitory behavior observed for the dependences of $K_i$ values for O-acyl-L-malates, 2-alkyl malonates (Fig. 6), and α,ω-alkylene dimalonates (Fig. 7) on $n$ (at $n > 3$) suggests that similar parts of aliphatic chains bind at the same regions of the transporter channel.

For O-acyl-L-malates and 2-alkyl malonates the dependences of $K_i$ values on $n$ were equidistant and there was "ideal correspondence" not only between linear parts but also between the coordinates of the bending points (see Fig. 6). Binding of an extended fragment ($n$ ranging from 8 to 17) of aliphatic chain of O-stearoyl-L-malate or 2-heptadecyl malonate provides 50-60% of the whole energy required for inhibitor binding at the active site. However, carboxyl groups of O-acyl-L-malate have more distant position (by 0.318 nm) from the first carbon atom of the aliphatic substituent than that in corresponding 2-alkyl malonate. Consequently, in the "relaxed" conformation a head of the acyl derivative may be positioned more distantly (by 2.34 aliphatic bond ($n$) length) from the large lipophilic area firmly anchoring the tail of this derivative. This suggests existence of two closely located malate and malonate putative binding sites. In this case, simultaneous binding of a bifunctional inhibitor at these two sites would be more effective than binding at one site (by $2\log K_i$ for malonate). However, in reality the $K_i$ values for dimalonate and 1,2-ethylydene dimalonate of 0.50 and 0.53 mM, respectively, were comparable with $K_i$ value for malonate (0.35 mM) [29]. This suggests a common binding site for both substrates in the active site of the dicarboxylate transporter.

It seems unlikely that malate binding instead of malonate would cause such a conformational change in the transporter molecule that would result in a shift of the polar zone and extended lipophilic regions of the transporter channel along the channel axis without changes in their sizes. For example, after conversion of aspartate/glutamate antiporter into nonspecific pore, the activation energy of this transporter remained unchanged [30]. This means that substrate binding has a minor contribution to the activation energy.

If binding sites for "heads" and "tails" of both series of these inhibitors coincide, acyl malate has to undergo rotation along its ester bond in the active site of the transporter. Bonds between the first carbon atom of malate carboxyl group and the first carbon atom of the substituent form a ring-shaped structure and so the distance between the line linking carboxyl groups and the first carbon atom of the aliphatic substituent positioned between them becomes equal to the distance between correspon-

ding groups of 2-alkyl malonates. (This was modeled using the Chemoffice program, MM2). Such conformational change may decrease affinity of all O-acyl-L-malates compared with 2-alkyl malonates (Fig. 6). The ring-shaped conformation also requires a relatively large space. This hypothesis is indirectly supported by known inhibitory activity of dicarboxylates with various distances between carboxyl groups (oxalate, malonate, succinate, glutarate, and adipinate) toward the transporter [31].

Certain experimental data support the existence of a large active site space closely located to the substrate-binding site. The transporter exhibits similar affinity for malonate, 2-methyl malonate, and 2,2-dimethyl malonate (Table 1). Similar affinity of the transporter to O-acyl-L and D-malates (Table 2) suggests some movement of a side group binding the L-hydroxyl group to amino acid residue-free space near cationic groups involved in substrate binding. In contrast to the substrate binding environment of succinate dehydrogenase, relatively low affinity of dicarboxylate transporter to substrate probably does not require multicentered interactions and rigidly configured tight environment. In contrast to transporter inhibition, succinate dehydrogenase inhibition by 2-methyl malonate was significantly lower (Table 1).

Lack of a sharp increase in inhibitory potency (affinity) for 1,6-hexylene dimalonate compared with dimethylmalonate and 1,2-ethylene dimalonate suggests that the transporter channel polar zone separating the large and small lipophilic areas does not contain cationic groups. Thus, the transporter channel lacks an intermediate substrate-binding site.

The dependence of $K_i$ value for α,ω-alkylene dimalonates and 2-alkyl malonates on the number of carbon atoms in the aliphatic chain is characterized by the bend point at $n \sim 7$ (Fig. 7). This suggests the existence of a common substrate-binding site for malonate "heads". The $K_i$ value for 2-alkyl malonate is lower than that of corresponding bifunctional inhibitor (Fig. 7). Lower dimalonates probably do not bind to the small lipophilic area of the transporter channel. The narrow transporter channel may also "create" steric problems for massive malonic group at the ω-position of all dimalonates.

The transporter channel has enough space for aliphatic chain in the region of the large lipophilic area. The following experimental data support this suggestion. The dependence of $K_i$ values for succinate oxidase on the carbon atom number in the aliphatic chain of inhibitors in the zone of the large lipophilic area (Fig. 6) and partition coefficient ($R_n$) in the system octanol/water (Fig. 8) are described by the linear equations $\log K_i = -0.38n + 1.41$ and $\log R = 0.416n - 3.46$, respectively. The coefficient values at $n$ have similar values in both equations. Consequently, energy for interaction of a methylene unit of the aliphatic chain of inhibitors ($\Delta\Delta G = RT\Delta\log K_i$) with amino acid residues lining this zone of the transporter channel is determined only by lipophilic interactions ($\Delta\Delta G = RT\Delta\log R_i$). There are no steric obstacles, which would reduce this value during interaction between transporter and inhibitor.

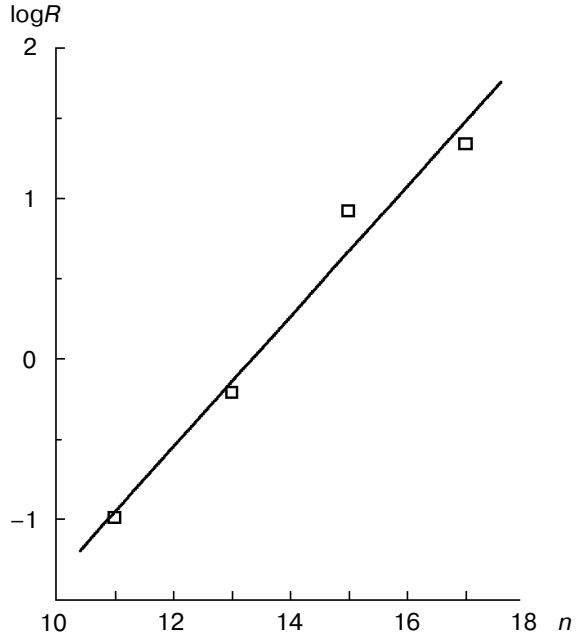


**Fig. 8.** Dependence of partition coefficient ($R$) in the system octanol/water on the number of carbon atoms ($n$) in the aliphatic chain of O-acyl-L-malates. Conditions: 10 mM potassium phosphate buffer, pH 7.2, was used as the aqueous phase.

Thus, results of comparative dicarboxylate transporter active site probing are well described by the following model: the L-malate-stereospecific single-substrate-binding site contains two cationic groups. It is located in a large space of the transporter molecule, whereas two lipophilic areas and the hydrophilic region separating these sites are located in the narrow channel formed by lipophilic transmembrane segments. The large lipophilic area acts as a gate preventing penetration of water molecules through the channel. The transporter oscillates between two distinct conformations in which the active site is faced (and susceptible) to mitochondrial matrix or to cytoplasm only. The transporter–inhibitor complex probably fixes the matrix-oriented conformation. The aliphatic chain of an inhibitor molecule binds at the semi-channel between the transporter substrate-binding site and the region exposed into the cytoplasm (*in vivo*). This semi-channel is narrowed and it does not contain water. Perhaps, dehydration of the additional malonic group of α,ω-alkylene dimalonates during complex formation causes delay in slowing steady state rate for transport inhibition by these bifunctional inhibitors.

In the opened active site exchange between free and bound substrate can occur. After transition of the active site into the alternative state, the active site becomes susceptible for free substrate molecules at the opposite side

of the mitochondrial membrane. Such mode provides exchange transport mechanism (antiport). Such states fixed by carboxyatractylate and bongkrekic acid have been describes for adenylate transporter [21, 32].

The proposed model and our approach for inhibitory analysis help better concretization of tasks on elucidation of putative role of uncharged hydrophilic residues of transmembrane lipophilic segments. In rat dicarboxylate transporter, these include Ser11, Ser67, Ser163, Ser199, and Ser200 [3]. The residues Ser11, Ser67, Ser163, and Ser200 are invariant for five organisms (mouse [2], rat [3], *Caenorhabditis elegans* nematode [3], *Saccharomyces cerevisiae* yeast [4], and man [5]). The existence of only one "polar" plateau in the lipophilic profile (dependence of $K_i$ value for the inhibition of mitochondrial succinate oxidase by inhibitor on the number of carbon atoms in the aliphatic chain) probably suggests that some but not all (of five) serine residues are exposed into the semi-channel between the substrate-binding site and the region of the transporter molecule exposed to the cytoplasm. Sequential point substitution of these residues for nonpolar residue(s) might reveal the putative residue responsible for the polar zone in this channel and also the residue responsible for transporter stereospecificity with respect to malate. Active site probing will help positioning of the substitution-carrying segment versus substrate-binding site and identify the surface of the transmembrane segment exposed into the channel. In accordance with α-helical pitch, each fourth/fifth residue of the primary structure from the identified residue will be also exposed into the channel. Point mutations made in primary structures of mitochondrial citrate [10] and α-ketoglutarate [11] transporters revealed that only one of six transmembrane segments of the transporter molecule contained functionally important conservative arginine residues. The authors assumed that an arginine residue of this segment was unquestionably exposed into the channel, and they demonstrated that each fourth residue from it became susceptible for water-soluble modifying agent after mutation for Cys [11, 33].

These authors investigated "opened" conformation of the channel whereas we studied "closed" conformation. X-Ray data obtained for the only member of the family of mitochondrial transporters [7] revealed that external ends of segments form the opened semi-channel whereas internal ends form the closed one. Lipophilicity of the internal semi-channel does not exclude existence of water-susceptible external semi-channel as Marty et al. suggested [12] and *vice versa*.

Thus, our approach of lipophilic profile scanning of the dicarboxylate transporter active site may result in imaging of its 3D-structure. More than 50 X-ray structures of hydrophilic substrate transporters are known to date [34], but only some of them have reasonably good resolution (1.2 Å) required for identification of the amino acid residues lining the transporter channel [34]. Ion pathway in the potassium channel [35] and ammonium ion pathway [36] in the bacterial ammonium ion transporter have the lining formed by hydrophobic amino acid residues, whereas in opened state the acetylcholine-dependent synaptic channel contains a significant number of polar residues [37]. It remains unclear whether channel functioning is accompanied by change in lipophilicity degree.

It is possible that the substrate-binding site involved in phosphate and phenyl phosphate binding [38], which is noncompetitive with respect to succinate and malate, is located outside the transporter channel transferring succinate, malonate, and malate. We can suggest the dicarboxylate transporter exists in two conformational states, phosphate-transferring and malate-transferring ones. Only the malate-transferring conformer binds butyl malonate [38] and is investigated using the molecular probes, malate competitors, used on our work.

This work was supported by a grant from the Russian Foundation for Basic Research (grant No. 04-04-49670).

## REFERENCES

1. Palmieri, L., Runswick, M. J., Fiermonte, G., Walker, J. E., and Palmieri, F. (2000) *J. Bioenerg. Biomembr.*, **32**, 67-77.
2. Das, K., Lewis, R. Y., Combatsiaris, T. P., Lin, Y., Shapiro, L., Charron, M. J., and Scherer, P. E. (1999) *Biochem. J.*, **344**, 313-320.
3. Fiermonte, G., Palmieri, L., Dolce, V., Larossa, F. M., Palmieri, F., Runswick, M. J., and Walker, J. E. (1998) *J. Biol. Chem.*, **273**, 24754-24759.
4. Xu, Y., Kakniashvili, D. A., Gremse, D. A., Wood, D. O., Walters, D. E., Mayor, J. A., and Kaplan, R. S. (2000) *J. Biol. Chem.*, **275**, 7117-7124.
5. Fiermonte, G., Dolce, V., Arrigoni, R., Runswick, M. J., Walker, J. E., and Palmieri, F. (1999) *Biochem. J.*, **344**, 953-960.
6. Kaplan, R. S., Mayor, J. A., and Wood, D. O. (1993) *J. Biol. Chem.*, **268**, 13682-13690.
7. Pebay-Peyroula, E., Dahout-Gonzalez, C., Kahn, R., Trezequet, V., Lauquin, G. J.-M., and Brandolin, G. (2003) *Nature*, **426**, 39-44.
8. Sholtz, K. F., Mamaev, D. V., Bondarenko, D. I., and Lagutina, L. S. (1990) *Biokhimiya*, **55**, 1832-1840.
9. Sholtz, K. F., Bondarenko, D. I., and Mamaev, D. V. (1993) *FEBS Lett.*, **327**, 54-56.
10. Xu, Y., Kakniashvili, D. A., Gremse, D. A., Wood, D. O., Walters, D. E., Mayor, J. A., and Kaplan, R. S. (2000) *J. Biol. Chem.*, **275**, 7117-7124.
11. Stipani, V., Cappello, A. R., Daddabbo, L., Natuzzi, D., Miniero, D. V., Stipani, I., and Palmieri, F. (2001) *Biochemistry*, **40**, 15805-15810.
12. Marty, I., Brandolin, G., Gagnon, J., Brasseur, R., and Vignais, P. V. (1992) *Biochemistry*, **31**, 4058-4065.
13. Sholtz, K. F., Mamaev, D. V., and Gladkikh, A. G. (1987) *Dokl. Akad Nauk SSSR*, **294**, 1509-1514.
14. Bisaccia, F., de Palma, A., Dierks, T., Kramer, R., and Palmieri, F. (1993) *Biochim. Biophys. Acta*, **1142**, 139-145.

15. Majima, E., Takeda, M., Miki, S., Shinohara, Y., and Terada, H. (2002) *J. Biochem.*, **131**, 461-468.
16. Mosolova, I. A., Gorskaya, I. A., Sholtz, K. F., and Kotelnikova, A. V. (1971) *Vopr. Med. Khim.*, **17**, 286-301.
17. Pedersen, P. L., Greenawalt, J. W., Reynafarje, B., Hullihen, J., Decker, G. L., Soper, J. W., and Bustamante, E. (1978) *Meth. Cell Biol.*, **20**, 411-488.
18. Goa, J. (1953) *Scand. J. Clin. Lab. Invest.*, **5**, 218-222.
19. Sholtz, K. F., and Ostrovsky, D. N. (1975) in *Methods of Modern Biochemistry* (Kretovich, V. L., and Sholtz, K. F., eds.) [in Russian], Nauka, Moscow, pp. 52-58.
20. Sholtz, K. F., and Mamaev, D. V. (1985) *Biokhimiya*, **50**, 1877-1883.
21. Terada, H. (1975) *Biochim. Biophys. Acta*, **387**, 519-532.
22. Bondarenko, D. I., Aliverdyeva, D. A., Mamaev, D. V., and Sholtz, K. F. (2004) *Dokl. Ros. Akad. Nauk*, **399**, 693-695.
23. Heirwegh, K. P. M., Meuwissen, J. A. T. P., Vermeier, M., and de Smedt, H. (1988) *Biochem. J.*, **254**, 101-108.
24. Bondarenko, D. I., Mamaev, D. V., and Sholtz, K. F. (1996) *Dokl. Ros. Akad. Nauk*, **349**, 408-410.
25. Kaprelyantz, A. S., Nikiforov, V. V., Miroshnikov, A. I., Snezhkova, L. T., Eremin, V. A., and Ostrovsky, D. A. (1977) *Biokhimiya*, **42**, 329-337.
26. Solov'eva, N. A., Kotelnikova, A. V., Miroshnikov, A. I., and Snezhkova, L. T. (1974) *Biokhimiya*, **39**, 1081-1085.
27. Passarella, S., and Quagliariello, E. (1976) *Biochimie*, **58**, 989-1001.
28. Indiveri, C., Capobianco, L., and Palmieri, F. (1988) *Ital. J. Biochem.*, **37**, 321A-323A.
29. Indiveri, C., Prezioso, G., Dierks, T., Kramer, R., and Palmieri, F. (1993) *Biochim. Biophys. Acta*, **1143**, 310-318.
30. Herick, K., and Kramer, R. (1995) *Biochim. Biophys. Acta*, **1238**, 63-71.
31. Passarella, S., Palmieri, F., Genchi, G., Stipani, I., and Quagliariello, E. (1972) *Boll. Soc. Ital. Biol. Sper.*, **48**, 341-345.
32. Klingenberg, M. (1989) *Arch. Biochem. Biophys.*, **270**, 1-14.
33. Kaplan, R. S., Mayor, J. A., Brauer, D., Kotaria, R., Walters, D. E., and Dean, A. M. (2000) *J. Biol. Chem.*, **275**, 12009-12016.
34. Dahl, S. G., Sylte, I., and Ravna, A. W. (2004) *J. Pharmacol. Exp. Ther.*, **309**, 853-860.
35. Jiang, Y., Lee, A., Chen, J., Ruta, V., Cadene, M., Chait, B. T., and MacKinnon, R. (2003) *Nature*, **423**, 33-41.
36. Andrade, S. L., Dickmanns, A., Ficner, R., and Einsle, O. (2005) *Proc. Natl. Acad. Sci. USA*, **102**, 14994-14999.
37. Miyazawa, A., Fujiyoshi, Y., and Unwin, N. (2003) *Nature*, **423**, 949-955.
38. Bisaccia, F., Indivery, C., and Palmiery, F. (1988) *Biochim. Biophys. Acta*, **933**, 229-240.